Impact of surface plasmon polaritons on photorefractive effect in dye doped liquid crystal cells with ZnSe interlayers

Tingyu Xue, Hua Zhao, Cuiling Meng, Jiayin Fu, and Jingwen Zhang*

Department of Physics, Harbin Institute of Technology, Harbin, 150001, China
jingwenz@hit.edu.cn

Abstract: Great impact of surface plasmon polaritons (SPPs) on photorefractive effect in ZnSe/liquid crystal interface was observed and studied in dye pyrromethane 597 doped 4,4'-n-pentylcyanobiphenyl (5CB) liquid crystal (LC) cells sandwiched with ZnSe coated ITO glass plates. Locally electrostatic modification of ZnSe in charge carrier density makes possible visible light excitation of SPPs in the LC/ZnSe interfaces. A tentative physical picture of SPP mediation was proposed in elucidating associated findings, including photoinduced scattering enhancement at low electric field and then reduction at high field, stepwise up- and down-turns in exponential gain coefficient, and 2D diffraction patterns. This work may open a new way toward tunable low-loss visible excitation of SPPs for plasmonic applications, specifically for organic plasmonics.

OCIS codes: (090.5694) Real-time holography; (240.6680) Surface plasmons; (190.4360) Nonlinear optics, devices; (160.3710) Liquid crystals.

References and links

1. O. Ostroverkhova and W. E. Moerner, "Organic photorefractives: mechanisms, materials, and applications," Chem. Rev. **104**(7), 3267–3314 (2004).
2. S. Tay, P.-A. Blanche, R. Voorakaranam, A. V. Tunç, W. Lin, S. Rokutanda, T. Gu, D. Flores, P. Wang, G. Li, P. St Hilaire, J. Thomas, R. A. Norwood, M. Yamamoto, and N. Peyghambarian, "An updatable holographic three-dimensional display," Nature **451**(7179), 694–698 (2008).
3. P.-A. Blanche, A. Bablumian, R. Voorakaranam, C. Christenson, W. Lin, T. Gu, D. Flores, P. Wang, W.-Y. Hsieh, M. Kathaperumal, B. Rachwal, O. Siddiqui, J. Thomas, R. A. Norwood, M. Yamamoto, and N. Peyghambarian, "Holographic three-dimensional telepresence using large-area photorefractive polymer," Nature **468**(7320), 80–83 (2010).
4. H. Zhao, C. Lian, X. Sun, and J. W. Zhang, "Nanoscale interlayer that raises response rate in photorefractive liquid crystal polymer composites," Opt. Express **19**(13), 12496–12502 (2011).
5. F. Simoni and L. Lucchetti, "Photorefractive effects in liquid crystals," in *Photorefractive Materials and Their Applications 2* P. Günter and J-P. Huignard, eds. (Springer, 2007, pp. 571–605)
6. I. C. Khoo, "Nonlinear optics of liquid crystalline materials," Phys. Rep. **471**(5-6), 222–267 (2009).
7. J. Zhang, V. Ostroverkhov, K. D. Singer, V. Reshetnyak, and Y. Reznikov, "Electrically controlled surface diffraction gratings in nematic liquid crystals," Opt. Lett. **25**(6), 221–416 (2000).
8. X. Sun, Y. Pei, F. Yao, J. Zhang, and C. Hou, "Optical amplification in multilayer photorefractive liquid crystal films," Appl. Phys. Lett. **90**(20), 201115 (2007).
9. X. Sun, F. Yao, Y. Pei, and J. Zhang, "Light controlled diffraction gratings in C_{60}-doped nematic liquid crystals," J. Appl. Phys. **102**(1), 013104 (2007).
10. I. C. Khoo, "The infrared optical nonlinearities of nematic liquid crystals and novel two-wave mixing processes," J. Mod. Opt. **37**(11), 1801–1813 (1990).
11. F. Poisson, "Nematic liquid crystal used as an instantaneous holographic medium," Opt. Commun. **6**(1), 43–44 (1972).
12. S. Bartkiewicz, A. Miniewicz, B. Sahraoui, and F. Kajzar, "Dynamic charge-carrier-mobility-mediated holography in thin layers of photoconducting polymers," Appl. Phys. Lett. **81**(20), 3705–3707 (2002).
13. L. Sznitko, A. Anczyowska, J. Mysliwiec, and S. Bartjiewicz, "Influence of grating period on kinetic of self-diffraction in nematic liquid crystal panel with photoconducting polymeric layer," Appl. Phys. Lett. **96**(11), 111106 (2010).

#214106 - $15.00 USD Received 23 Jun 2014; revised 8 Aug 2014; accepted 10 Aug 2014; published 21 Aug 2014

14. Y. Williams, K. Chan, J. H. Park, I. C. Khoo, B. Lewis, and T. E. Mallouk, "Electro-optical and nonlinear optical properties of semiconductor nanorod doped liquid crystals," Proc. SPIE **5936**, 593613 (2005).
15. V. Boichuk, S. Kucheev, J. Parka, V. Reshetnyak, Y. Reznikov, I. Shiyanoskaya, K. D. Singer, and S. Slussarenko, "Surface-mediated light-controlled Friedericksz transition in a nematic liquid crystal cell," J. Appl. Phys. **90**(12), 5963–5967 (2001).
16. M. Kaczmarek, A. Dyadyusha, S. Slussarenko, and I. C. Khoo, "The role of surface charge field in two-beam coupling in liquid crystal cells with photoconducting polymer layers," J. Appl. Phys. **96**(5), 2616–2623 (2004).
17. H. Zhao, C. Lian, F. Huang, T. Xue, X. Sun, Y. K. Zou, and J. Zhang, "Impact of grating spacing and electric field on real time updatable holographic recording in nanoscale ZnSe film assisted liquid crystal cells," Appl. Phys. Lett. **101**(21), 211118 (2012).
18. C. Lian, H. Zhao, Y. Pei, X. Sun, and J. Zhang, "Fast response beam coupling in liquid crystal cells sandwiched between ZnSe substrates," Opt. Express **20**(14), 15843–15852 (2012).
19. C. H. Ahn, A. Bhattacharya, M. Di Ventra, J. N. Eckstein, C. D. Frisbie, M. E. Gershenson, A. M. Goldman, I. H. Inoue, J. Mannhart, A. J. Millis, A. F. Morpurgo, D. Natelson, and J.-M. Triscone, "Electrostatic modification of novel materials," Rev. Mod. Phys. **78**(4), 1185–1212 (2006).
20. S. Hayashi and T. Okamoto, "Plasmonics: visit the past to know the future," J. Phys. D Appl. Phys. **45**(43), 433001 (2012).
21. U. Fano, "The theory of anomalous diffraction gratings and of quasi-stationary waves on metallic surfaces (Sommerfeld's waves)," J. Opt. Soc. Am. **31**(3), 213–222 (1941).
22. I. Packrand, "Resonance anomalies in the light intensity reflected at silver grating with dielectric coatings," J. Phys. D: Appl. Phys. **9**, 2423–2432 (1976).
23. J. Hägglund and F. Sellberg, "Reflection, absorption and emission of light by opaque optical gratings," J. Opt. Soc. Am. B **56**, 1031–1040 (1966).
24. Y. Teng and E. Stern, "Plasma radiation from metal grating surfaces," Phys. Rev. Lett. **19**(9), 511–514 (1967).
25. R. H. Ritchie, E. T. Arakawa, J. J. Cowan, and R. N. Hamm, "Surface-plasmon resonance effect in grating diffraction," Phys. Rev. Lett. **21**(22), 1530–1533 (1968).
26. D. Maystre, "Diffraction gratings: An amazing phenomenon," C. R. Phys. **14**(4), 381–392 (2013).
27. M. Kauranen and A. V. Zayats, "Nonlinear plasmonics," Nat. Photonics **6**(11), 737–748 (2012).
28. A. E. Rider, K. Ostrikov, and S. A. Furman, "Plasmas meet plasmonics," Eur. Phys. J. D **66**(9), 226 (2012).
29. A. V. Zayats, I. I. Smolyaninov, and A. A. Maradudin, "Nano-optics of surface plasmon polaritons," Phys. Rep. **408**(3-4), 131–314 (2005).
30. A. Poddubny, I. Iorsh, P. Belov, and Yu. Kivshar, "Hyperbolic metamaterials," Nat. Photonics **7**(12), 948–967 (2013).
31. L. Huang, X. Chen, H. Mühlenbernd, H. Zhang, S. Chen, B. Bai, Q. Tan, G. Jin, K. Cheah, C. Qiu, J. Li, T. Zentgraf, and S. Zhang, "Three-dimensional optical holography using a plasmonic metasurface," Nat. Commun. **4**, 2808 (2013).
32. P. R. West, S. Ishii, G. V. Naik, N. K. Emani, V. M. Shalaev, and A. Boltasseva, "Searching for better plasmonic materials," Laser Photon. Rev. **4**(6), 795–808 (2010).
33. H. Kim, C. M. Gilmore, A. Piqué, J. S. Horwitz, H. Mattoussi, H. Murata, Z. H. Kafafi, and D. B. Chrisey, "Electrical, optical, and structural properties of indium-tin-oxide thin films for organic light-emitting devices," J. Appl. Phys. **86**(11), 6451–6461 (1999).
34. M. C. Cross and P. C. Hohenberg, "Pattern formation outside of equilibrium," Rev. Mod. Phys. **65**(3), 851–1112 (1993).
35. S. J. Elston and J. R. Sambles, "Surface plasmon-polaritons on an anisotropic substrate," J. Mod. Opt. **37**(12), 1895–1902 (1990).
36. K. R. Daly, S. Abbott, G. D'Alessandro, D. C. Smith, and M. Kaczmarek, "Theory of hybrid photorefractive plasmonic liquid crystal cells," J. Opt. Soc. Am. B **28**(8), 1874–1881 (2011).
37. B. I. Sturman, S. G. Odoulov, and M. Yu. Goulkov, "Parametric four-wave processes in photorefractive crystals," Phys. Rep. **275**(4), 197–254 (1996).

1. Introduction

Searching for new polymer [1–4] and liquid crystal (LC) [5–9] nonlinear optical materials and optimizing existing ones are of growing foci in optical field, driven by a broad spectrum of applications, especially for real time holography. With photoconductor substrates [10], interlayers [11–13], and nanorods [14] in modifying LC cells, few to tens millisecond response times were demonstrated. In the past, surface dominant photorefractive effects were demonstrated and studied in LC cells [7,15–18]. It is evident that charge carrier transportation and accumulation near the photoconductor/LC interface are behind most interesting phenomena observed [12,13,15–18]. When a great number of electrons are accumulated near a photoconductor/LC interface, the skin layer of the photoconductor can be swarmed by charge carriers (electrons or holes) upon applying an electric field. Based on the physical picture of electrostatic modification [19], the conductivity of the photoconductor could be

#214106 - $15.00 USD Received 23 Jun 2014; revised 8 Aug 2014; accepted 10 Aug 2014; published 21 Aug 2014

boosted greatly. Consequently, the plasma frequency of the photoconductor can be shifted towards short wave side [20]. This blue-end-shifting is of prime importance in plasmonics. Metallic gratings were extensively used in energy coupling between visible radiation and surface plasmon polaritons (SPPs) [21–25], playing key roles in nanophotonics [20,26–31]. To circumvent inherent huge loss in metallic materials, along another line, researchers are actively searching alternative low-loss nonmetal plasmonic materials [32]. Among others, well conductive n-type semiconductors were found favorable in lowering losses [32,33]. It is known that phase gratings can be written in a nonlinear material [6]. Therefore, in a layered structure of plasmonic and nonlinear optical materials, SPP excitation and energy coupling between light radiation and SPPs can be mediated by phase gratings, instead of metallic gratings. Recently, we have observed interesting phenomena in dye doped 4,4'-n-pentyl-cyanobiphenyl LC cells, fabricated with n-type semiconductor ZnSe coated ITO glass plates. The observations can be explained with excitation of SPPs and energy coupling between SPPs and visible radiation. In dye pyrromethane 597 doped LC cells, stepwise gain coefficients ranging from –400 to 400 cm^{-1} were obtained with increasing applied field and the energy coupling direction was doping concentration dependent. Strikingly, a very strong scattering nearly depleted transmitted laser beams at a relatively low applied field. After a turning point, however, the scattering light was reduced when applied field was raised further. Based on SPP excitation and its mediation in energy coupling process, both the gain coefficient and transmitted power dependences on the applied field can be explained satisfactorily. Moreover, 2D hexagonal diffraction patterns observed from lighter dye doped LC cells supported the physical picture proposed. By measuring the charge accumulation in the interfaces, it arrives that locally electrostatic modification of ZnSe in charge carrier density makes possible visible light excitation of SPPs in the LC/ZnSe interfaces. This study could serve as guidance in designing tunable, low-loss plasmonic systems and it is also of significance for nonlinear optics research. We report our work as follows.

2. Experimental and discussion

2.1 Two wave mixing experiment

The nematic LC material 4,4'-n-pentylcyanobiphenyl (5CB) in making LC cells was purchased from Merck, and the dye pyrromethane 597 from Exciton. The photoconductive ZnSe films were coated on ITO glass plates directly by electron beam deposition. The structure of an LC cell and the experimental configuration of two wave mixing (TWM) are illustrated in Fig. 1(a). The ZnSe films on top of two ITO glass serve as not only photoconductive layer, but also alignment layer. In preparing the liquid crystal cell, a few nm uneven morphology of the ZnSe coating plays the aligning role in forming a high-quality homeotropical cell, as stated in Ref. 17, along with the advantage of this approach offers. Using a typical oblique geometry, the LC cell was tilted at angle $\varphi = 45°$ to the bisector of writing beams 1 and 2. The thickness of the LC cell was set as $d = 6.35$ μm with polyester spacers. A continuous diode pumped solid state laser at 561 nm (Cobolt Samba 100) was used as the coherent light source and p-polarized incident light was used throughout the work. The crossing angle of beams 1 and 2 was set at $\theta = 1.0°$, with the corresponding grating spacing $\Lambda = 18.7$ μm. The two writing beams were with equal powers, 5 mW. Growing energy coupling from one beam to the other was seen with increasing applied field in a 1.0 wt% dye doped LC cell. The gain coefficients were calculated according to $\Gamma = (\cos\varphi)/d \cdot \ln[(I_2 I_1')/(I_1 I_2')]$ and plotted in Fig. 1(b) against the applied voltage. Where I_1 and I_2 are the transmitted intensities without coupling, I_1' and I_2' the transmitted beam intensities with coupling, d the thickness of the sample, and φ the tilt angle of sample to the bisector of writing beams. Multiple measurements for TWM exponential gain coefficient were performed against applied field in many LC cells. The highest gain coefficient measured was 400 cm^{-1} from the LC cell. It is noted in the experiments that the coupling between the two beams was quite dynamic

#214106 - $15.00 USD Received 23 Jun 2014; revised 8 Aug 2014; accepted 10 Aug 2014; published 21 Aug 2014

although a vibration-proof table was employed. It is seen that at relatively low electric field the gain coefficient fluctuated above and below the zero line around ± 50 cm^{-1}. After 0.4 V/μm, the gain coefficient grew sharply until 0.6 V/μm. Over 0.8 V/μm, the gain experienced a slow downtrend till 1.6 V/μm. It was even interesting to see that the gain coefficient grew again after 1.7 V/μm. One notes that fluctuation of the gain coefficient was quite striking in the graph, judging from the big error bars. The TWM experiments were repeated with multiple cells and these results were well reproduced.

To see the contribution of the doping concentration of dye on the energy coupling and grating writing process, the dye doping concentration was diluted to be 0.5 wt%, 0.1 wt%, and 0.01 wt% by adding more LC material into the LC + dye solution. The dependence of the gain coefficient on the applied field in the LC cells with different doping concentrations were measured and shown in Fig. 1(a). One can see that the gain coefficients experienced negative values before turning positive. It is puzzling to see that for the slightest doping LC cell, the gain coefficient did not even turn to positive. In the previous work, we noticed similar energy transferring [17] without delving into the mechanism behind the finding. It is apparent that charge transferring and accumulation are associated with it. To get fuller picture about the complicated energy transferring process, we proceed to look at light scattering closely next.

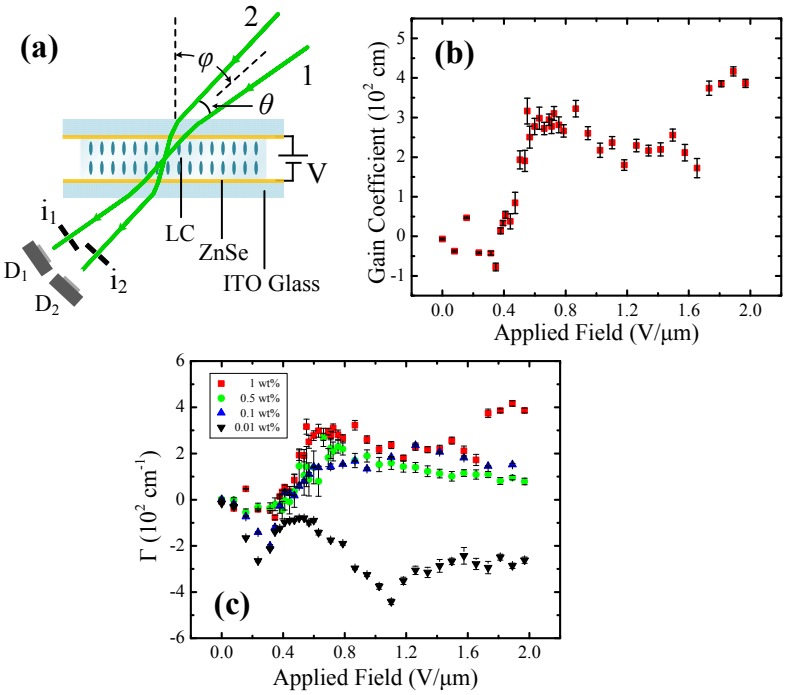

Fig. 1. (a) Schematic diagram for measuring transmitted powers with/without two beam coupling in LC cells with asymmetrical incident beams: Di are detectors, ii irises with 1.0 mm diameters, θ external cross angle between two beams, and V applied voltage; (b) The TWM exponential gain coefficient versus applied electric field; (c) Gain coefficient for samples with different doping concentration.

2.2 Transmitted intensity variation with applied field

To find the origin behind the intriguing observation in the TWM experiment, the transmitted powers of beams 1 and 2 were measured against applied field at three conditions: (1) beam 1 alone (marked with I_1, see Fig. 2(a)); (2) beam 2 alone (marked with I_2, Fig. 2(a)); and (3) beams 1 and 2 coexistence (marked with I_1' and I_2', Fig. 2(b)). One sees that beams 1 and 2 experienced great power drops at 0.39 V/μm, and the electric fields corresponding to the

#214106 - $15.00 USD Received 23 Jun 2014; revised 8 Aug 2014; accepted 10 Aug 2014; published 21 Aug 2014

lowest powers for transmitted beams differed slightly, around 0.6 V/μm. It was noted that the transmitted light became stronger after a turning point, while the applied electric field was increased continuously (Fig. 2(a) and 2(b)). This turning point was consistent to the Fredericks threshold of the liquid crystal. One puzzling thing was that the sharp declining of transmitted power (Fig. 2(a) and 2(b)) was coincident to the sharp increasing of exponential gain coefficient in Fig. 1(b). Moreover, the transmitted beams gradually regained their powers after the turning point until 1.6 V/μm, originating seemingly from moving away from the Fredericks transition, due to the stronger alignment of the liquid crystal to the applied field, resulting in the exponential gain coefficient in a slow downturn at same time. Finally, after the transmitted beams regaining full powers, the gain coefficient grew considerately. One thing deserves to be pointed out that the coefficients obtained in 0.01% doping LC cell were with opposite sign, hinting backward energy transferring, while the geometrical and optical conditions were all the same.

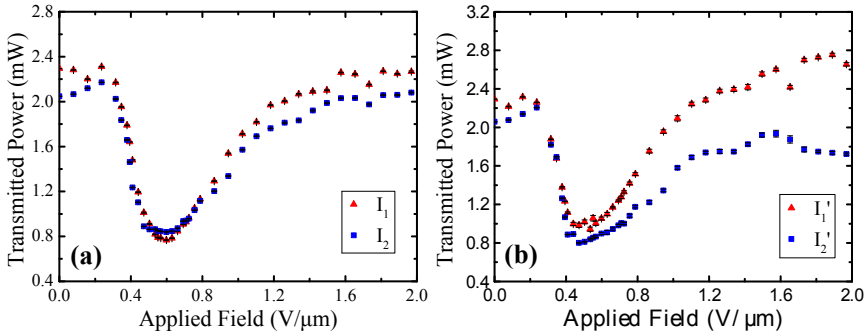

Fig. 2. Transmitted powers of beams 1 and 2 in the cases when (a) the beams were turning on one after another; (b) the beams were coexistent temporally.

2.3 Transmitted intensity variation with total power flux

One may wonder: why did the transmitted power experience so great a decline? To answer this question, one needs to take a look at the transmitted spots without the irises in the light path illustrated in Fig. 1(a). Four selected photographs taken at different electric fields are exhibited in Fig. 3(a). One sees that with increasing electric field the scattering increased remarkably, and this answers why the transmitted powers after irises were reduced. It is striking to see that after 0.6 V/μm the scattering reversed course. At 1.57 V/μm, the scattering shrank to that at 0.39 V/μm. This scattering's up- and down-turns imply there are at least two competing driving forces in determining the scattering. The first driving force—photorefractive effect—tends to increase scattering powers and distribution angles when the applied electric field was increased, since the light energy tends to be coupled into much weaker scattering beams. To find the second driving force, which tends to reduce light scattering, it would be informative if one checks total transmitted power difference between the two cases: (1) turning on beams 1 and 2 individually; (2) turning on both beams simultaneously (refer to Fig. 3(b)). One sees that there was a sharp peak around 0.4 V/μm, which coincided with the sharp decline of the transmitted powers (Fig. 2(a) and 2(b)). Apparently, doubling the incident power flux increased the scattering at relatively low electric field. Contrarily, at high electric field, the higher power flux sped up decreasing of the scattering. In photorefractive systems, higher incident power results in faster charge carrier generation and transportation, and hence alters the effective electric field. Therefore, to identify the second driving force, we will take a closer look at charge transportation and charge accumulation in the next section.

#214106 - $15.00 USD Received 23 Jun 2014; revised 8 Aug 2014; accepted 10 Aug 2014; published 21 Aug 2014

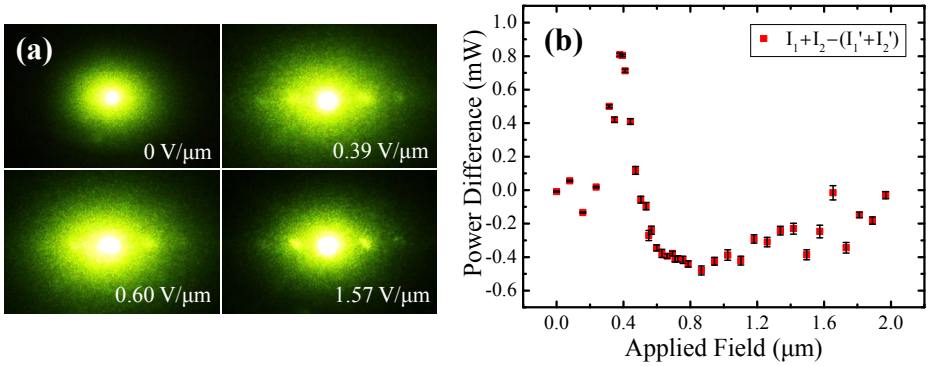

Fig. 3. (a) The scattering pattern variation of individual beam at different applied field intensities; (b) The influence of total flux of on the total transmitted power in the dye doped LC cell.

3. Theoretical consideration and further experimental confirmation

3.1 Charge accumulation, dark and photocurrents

As briefly stated in the introduction section, various intriguing phenomena observed in doped LC cells were intimately associated with charge carrier transportation and accumulation near the LC/photoconductor interfaces [7,12–18]. Indeed, the interesting findings in our previous works [17,18] motivated us to explore unknown mechanisms in the ZnSe/LC interface. While external field was applied on an LC cell, charge carriers were accumulated on the electrodes. When a ZnSe/LC interface was flooded with electrons, the effective electron density of the skin layer of ZnSe thin film was altered significantly due to electrostatic modulation [19]. In view of plasmonics, the plasma frequency (ω_p) of ZnSe layer could be shifted greatly towards short wave, since ω_p can be expressed as [33]

$$\omega_p = \sqrt{\frac{4\pi n_e e^2}{\varepsilon_0 \varepsilon_\infty m_e}} \tag{1}$$

where n_e is the electron density, e the charge of an electron, m_e the effective mass of electron, ε_∞ and ε_0 represent the dielectric constants of the medium and free space. One sees that if electron density is high enough, ω_p could be shifted well into visible regime.

To see how electrons can be accumulated near the ZnSe/LC interface and the amount accumulated, the current dynamics during turning on and shutting down of electric field/light were taken with a picoammeter (Keithley, model 6485) connected in series with a DC power supply and the LC cell used in the TWM experiment. The dark and photoinduced charge accumulation versus applied voltage is exhibited in Fig. 4(a). A typical charging dynamic curve is shown in the inset. The charge accumulation near the ZnSe/LC interface was calculated by integrating the total area enclosed by the jump lines (upon turning on electric field (laser light), decaying curves and dashed lines corresponding to the stable currents (Fig. 4(a)). Figure 4(b) shows that the stable dark- and photo-current are different. One thing should be mentioned here is that the dark charge accumulation and dark current were attributed to the entire electrode area of the LC cell (12 × 24 mm^2), whereas only a very small portion of the electrode (4 mm^2) was illuminated and hence contributed to the photocharge accumulation and photocurrent. Considering the area ratio 72, the photoinduced contributions were indeed great.

#214106 - $15.00 USD Received 23 Jun 2014; revised 8 Aug 2014; accepted 10 Aug 2014; published 21 Aug 2014

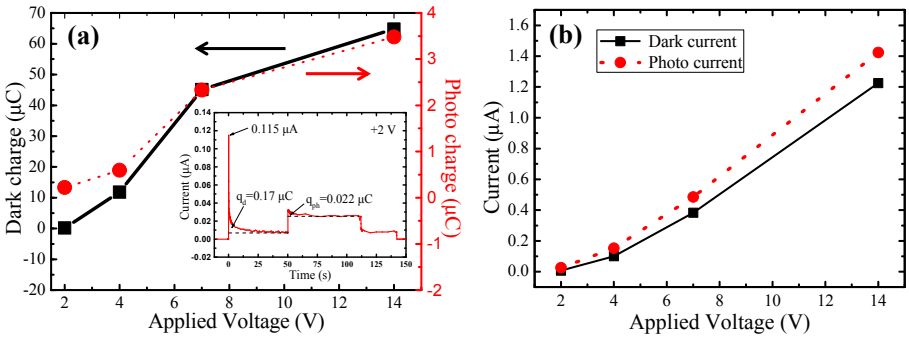

Fig. 4. (a) Total charge accumulation near ZnSe/LC interface in dark condition and extra charge accumulation under illumination of laser beam in 1.0 wt% dye doped sample; (b) Stable dark and photo current versus applied voltage. The lines serve as guide for eye.

3.2 A tentative physical model

From Fig. 4(a), it is seen that 0.17 to 64 μC electrons can be accumulated near the ZnSe/LC interface in 1.0 wt % dye doped sample with 2 to 14 V voltage applied. The amount of charge accumulation differs for different doping concentrations, but with the same order of magnitude. According to Eq. (1), the plasma response of the ZnSe will be shifted toward short wave side, and may reach visible region. Rough calculations were done as follows to estimate the magnitude of this blue-end shifting. The electron density in ZnSe layer before charge accumulation was calculate by using the relation [33]

$$\lambda_p(\mu\mathrm{m}) = 1.24e/(\hbar\omega_p) \tag{2}$$

together with Eq. (1). Here, $\hbar$ is reduced Planck constant. The cutoff wavelength λ_p was obtained by measuring the transmission spectrum of bulk ZnSe. Assuming the accumulated electrons were mostly squeezed into a very thin ZnSe layer adjacent to the LC layer, whose thickness is in the magnitude of Debye screen length (equal to $[\varepsilon_{sc}k_BT/(4\pi e^2 n_0)]^{1/2}$, ε_{sc}, k_B, T, e, and n_0 are semiconductor permittivity, Boltzmann's constant, temperature, charge of carrier, and the electron concentration, respectively), the added charge density can be calculate by considering the electrode area of LC cell and the amount of charge accumulation. Replace n_e in Eq. (1) with electron density after charge accumulation, the new plasma frequency and cutoff wavelength (or plasma wavelength) can be calculated according to Eq. (1) and Eq. (2) respectively. With the charge accumulation increased from 0.17 to 64 μC, the shifted plasma wavelength range from 6.2 to 0.34 μm, covering indeed the visible regime

Therefore, mediated by the gratings written in the LC cells, SPPs at visible frequencies can be excited near ZnSe/LC interface on the cathode side (Fig. 5(a)). Because of the high sensitivity of photorefractive effect, the weak scattering light in LC cells can be amplified by writing myriad gratings. Consequently, those phase gratings diffract incident light into various high orders. Similar to the metal grating used in the past [20,21,26], the phase gratings can supply quasi-wavevectors of $m(2\pi/\Lambda)$ to the x-component of the incident light wavevector k_{xin} to satisfy phase match condition, where Λ is spatial period of a phase grating. The energy of incident light is transferred to the SPPs by diffraction. The condition for SPP excitation by the phase grating is expressed as [20]

$$k_{SPP} = k_{xin} + \Delta k_x = k_{xin} + m\frac{2\pi}{\Lambda}, \qquad m = \pm 1, \pm 2, \ldots, \tag{3}$$

where k_{SPP} is the vector of SPPs, determined by both dielectric function of the electrostatically modified photoconductor ZnSe and dielectric constant of the LC layer, and the order number m could be either positive or negative [20]. As illustrated in Fig. 5(a), the SPPs propagate in

#214106 - $15.00 USD Received 23 Jun 2014; revised 8 Aug 2014; accepted 10 Aug 2014; published 21 Aug 2014

both positive and negative directions of the x-axis. It is noted the charge carriers are accumulated on the ZnSe/LC interface, since ZnSe layer is semiconducting and hence the applied voltage dropped down across the dielectric LC layer. The plasmonic band structure in the ZnSe/LC system was computed according to Eq. (3) by schematically setting Λ = 18.7 μm and shown in Fig. 5(b). Note that the manifold dispersion curves fall within the radiation region between the two air light red lines, implying coupling between SPPs and light radiation are of two-way process. From the schematic graph of Fig. 5(b), it is seen the scattered beams which form small angles with the incident light write gratings with large spacing period Λ, and hence more dispersion curves are packed between the two light lines. Therefore, scattering with relatively small angles with the incident beam have greater chances to be amplified via backward coupling from SPPs to radiation. This is believed to be the second driving force which brings scattering light back to the incident light direction, while higher electric field pushing plasma frequency toward shorter waves. The grating spacing formed between the main beams and scattering beams are relatively large, while the grating spacing between scattering beams are relatively small, this make the SPPs couple more energy into the main beams than that into the scattering beams. Also because of the difference in the grating spacings, the energy coupling from the scattering beams to the SPPs are more than that from the main beams. Therefore, the scattering beam become weaker while the main beams stronger.

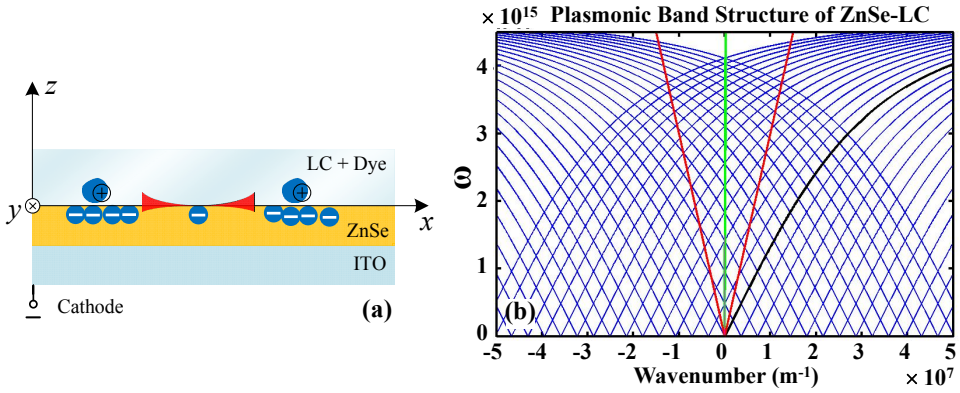

Fig. 5. (a) Schematic diagram illustrating carrier charge accumulation and excitation of SPPs near ZnSe/LC interface; (b) Schematic illustration of plasmonic structure of electrostatically modified ZnSe/LC interface.

3.3 Further experimental results

An intriguing finding in the slightest dye doped LC cell was believed to be an evidence to SPP excitation and energy transferring from SPPs to visible radiation. Without external feedback of any sort employed in previous works [34], 2D diffraction pattern was observed out of the LC cell. After illuminating with two writing beams, a grating was written. On the reflection side, over 18 diffraction orders were seen Fig. 6(a)). On the transmitted side, very clear 2D diffraction patterns appeared (Fig. 6(b)) and the distribution of the high orders changed over time. In the past, the SPP excitation in the interface between isotropic and anisotropic media were studied [35,36]. It is believed in the less dye doped LC cell, both the s-and p-polarized light can excite the SPPs in the Znse/LC interfaces. Therefore, 2D interference patterns were formed. Regarding 2D diffraction patterns, it is well known in photorefractive research community that primarily the phase matching condition defines the shape of the scattering pattern if parametric amplification is involved [37]. The light spots in the central row were of many diffraction orders. For those spots above and below the central row, they seemingly stem from energy coupling between crossed polarizations. However, the

#214106 - $15.00 USD Received 23 Jun 2014; revised 8 Aug 2014; accepted 10 Aug 2014; published 21 Aug 2014

ring-shaped diffraction lines were reduced and the bright spots were enhanced greatly, since the SPPs can only couple with the diffracted light of p-polarization. From another perspective, the modified ZnSe layer can serve as a thin mirror for visible light due to plasma excitation, which serves as the feedback needed for generating 2D diffraction patterns [34].

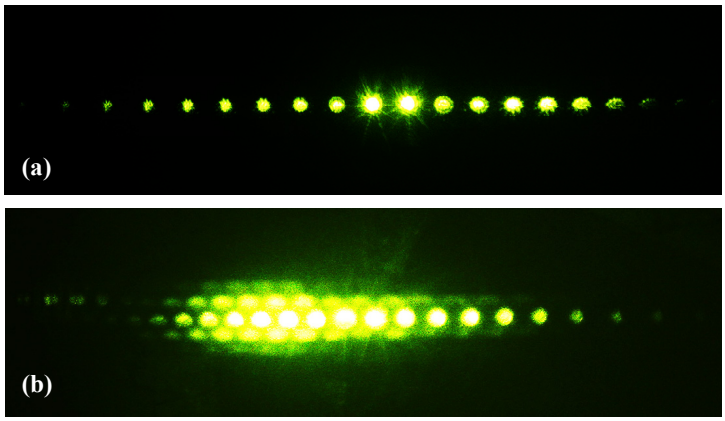

Fig. 6. (a) Reflected (b) 2D Transmitted diffraction pattern taken in a dye doped 5CB with 3 V voltage applied.

4. Conclusion

In conclusion, apparent SPP excitation was evidenced in dye doped 5CB LC cells made of ZnSe coated ITO glass plates and great impact on the photorefractive effect was analyzed and verified by experiments. The charge accumulation near the ZnSe/LC interfaces results in electrostatic modification of the plasma frequency toward visible wave, and this makes possible to excite SPPs in the visible band. Additionally, hexagonal transmitted patterns were observed and analyzed in the slightest dye doped LC cells. The findings could be used as guidance in designing low loss SPPs based devices and in designing fast response, low voltage operated holographic display. Since the charge accumulation is highly electric field and illumination dependent, the electrostatic modification approach opens a new way of exciting SPPs in a tunable way. This methodology itself is significant for plasmonics.

Acknowledgments

This work has been supported by the grant of National Natural Science Foundation of China under project No. 11174067. The authors are indebted to the Key Laboratory of Micro-Optics and Photonics Technology of Heilongjiang Province, Harbin, China, for full access to the facility.

#214106 - $15.00 USD Received 23 Jun 2014; revised 8 Aug 2014; accepted 10 Aug 2014; published 21 Aug 2014